

# Optimal preparation of the maximally entangled $W$ state of three superconducting gmon qubits

Dalton Jones<sup>1,2</sup> and Armin Rahmani<sup>2,3,4</sup>

<sup>1</sup>*Department of Physics and Astronomy, University of California, Los Angeles, California 90095, USA*

<sup>2</sup>*Department of Physics and Astronomy, Western Washington University, Bellingham, Washington 98225, USA*

<sup>3</sup>*Advanced Materials Science and Engineering Center,*

*Western Washington University, Bellingham, Washington 98225, USA*

<sup>4</sup>*Kavli Institute for Theoretical Physics, University of California, Santa Barbara, California 93106, USA*

(Dated: May 16, 2023)

Superconducting gmon qubits allow for highly tuneable quantum computing devices. Optimally controlled evolution of these systems is of considerable interest. We determine the optimal dynamical protocols for the generation of the maximally entangled  $W$  state of three qubits from an easily prepared initial product state. These solutions are found by simulated annealing. Using the connection to the Pontryagin’s minimum principle, we fully characterize the patterns of these “bang-bang” protocols, which shortcut the adiabatic evolution. The protocols are remarkably robust, facilitating the development of high-performance three-qubit quantum gates.

## I. INTRODUCTION

There have been numerous advances in creating coherent quantum systems [1–3] for information processing. Entanglement is a crucial resource in quantum information processing [4, 5]. Preparing maximally entangled states is thus of great interest. There are two fundamental ways of entangling three qubits, the Greenberger-Horne-Zeilinger states, and the  $W$  state [6, 7]. In this paper we focus on the optimally fast creation of  $W$  states of three qubits. The creation of these states has been studied in many contexts [8–15]. Due to the long coherence times and remarkable tunability, superconducting qubits provide an important platform for creating maximally entangled states [16–20]. The  $W$  states have been created using a fast three-qubit entangler gate in the Martinis lab [21]. However, the question of finding the optimal, i.e., fastest possible, unitary for the creation of the  $W$  state with the same existing quantum hardware remains open. Here we apply the theory of optimal control to this problem.

The superconducting architecture we focus on is known as the gmon qubit [22], which allows for precise time-dependent control of the inductively coupled qubits. High tunability enables us to perform tailored optimized unitary operations. One method for driving the system to a maximally entangled state is through the adiabatic evolution. We may reach the desired state adiabatically in timescales much larger than the scale set by the energy gap between the ground state and first excited state of the system. However, if the chosen trajectory of the time-dependent Hamiltonian contains a level crossing (or exceedingly small gap) between the ground state and first excited state, adiabatic evolution is infeasible. The system is likely to decohere before the completion of the adiabatic process. For an exact level crossing, the initial and final states may belong to different symmetry sectors, making it impossible to transform them into each other with a symmetry-preserving Hamiltonian. Consequently, we employ a different method, namely, optimal control, to efficiently evolve the system.

Optimal control techniques that shortcut the adiabatic evolution have been studied extensively [23–44]. Recently, we found optimal protocols for evolving a product state of two

gmon qubits into a maximally entangled singlet state of two qubits [45]. These solutions, confirmed by Pontryagin’s minimum principle, are bang-bang., i.e., a sequence of square pulses. They also substantially shortcut the adiabatic evolution. Here we generalize the results of Ref. [45] to a system of three gmon qubits. We find optimal solutions for preparing a maximally entangled state, known as the  $W$  state

$$|W\rangle = \frac{1}{\sqrt{3}}(|\downarrow\uparrow\downarrow\rangle + |\uparrow\downarrow\downarrow\rangle + |\downarrow\downarrow\uparrow\rangle), \quad (1)$$

from a product state.

We begin by performing numerical optimizations to minimize a cost function based on the difference between the final state of the system and the maximally entangled state (1). We then use Pontryagin’s Minimum principle to confirm and improve these solutions. Our solutions provide specific operations for optimally controlling a system of three gmon qubits, to quickly create the  $W$  state. Furthermore, these solutions bring us a step closer to understanding the structure of optimal control protocols.

## II. MODEL AND SETUP

The superconducting gmon qubit architecture [22] is described by a Hamiltonian with tuneable parameters. For the case of three qubits the Hamiltonian has the form:

$$H = B_1\sigma_1^z + B_2\sigma_2^z + B_3\sigma_3^z + J_{12}(\sigma_1^x\sigma_2^x + \sigma_1^y\sigma_2^y) + J_{23}(\sigma_2^x\sigma_3^x + \sigma_2^y\sigma_3^y) + J_{31}(\sigma_3^x\sigma_1^x + \sigma_3^y\sigma_1^y). \quad (2)$$

This Hamiltonian has six parameters corresponding to single-qubit fields and qubit-qubit couplings. We have not included  $\sigma^x$  and  $\sigma^y$  single-qubit operations, which simplifies both the experimental implementation and theoretical understanding of the problem. Setting these possible terms to zero limits the number of control parameters and conserves  $\sum_j \sigma_j^z$ , corresponding to the total number of photons in the device. We assume for simplicity that all parameters can be tuned as a function of time in the range:

$$0 \leq B_1(t), B_2(t), B_3(t), J_{12}(t), J_{23}(t), J_{31}(t) \leq \Lambda, \quad (3)$$

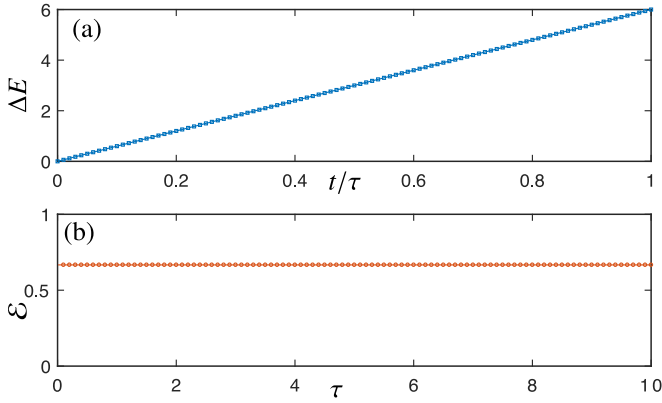


FIG. 1. (a) The energy gap for  $B_1 = B_2 = B_3 = 1 - t/\tau$  and  $J_{12} = J_{23} = J_{31} = t/\tau$  as a function of  $t/\tau$  indicating the initial degeneracy. (b) The error function  $\mathcal{E} = 2/3$  for the final state is independent of the total time, showing the failure of the adiabatic transformation.

where  $\Lambda$  sets the energy scale of the system. Hereafter, we use  $\Lambda = 1$  and also set  $\hbar$  to one.

The target state is

$$|\psi_{\text{target}}\rangle = |W\rangle, \quad (4)$$

where the up and down spins are eigenstates of  $\sigma^z$  ( $\sigma^z|\uparrow\rangle = |\uparrow\rangle$  and  $\sigma^z|\downarrow\rangle = -|\downarrow\rangle$ ), and  $\sigma^{x,y,z}$  are the Pauli matrices.

The Hamiltonian (2) preserves the total spin in the  $z$  direction and the target state has  $\sum_{j=1}^3 \sigma_j^z = -1$ . We thus focus on the three-dimensional Hilbert space corresponding to this sector. The Hamiltonian in this sector can be written as

$$H = \begin{pmatrix} B_1 + B_2 - B_3 & -2J_{23} & -2J_{31} \\ -2J_{23} & B_1 - B_2 + B_3 & -2J_{12} \\ -2J_{31} & -2J_{12} & B_2 - B_1 + B_3 \end{pmatrix}. \quad (5)$$

The target state (4) is a ground state of the Hamiltonian (2) for, e.g.,  $J_{12}, J_{23}, J_{31} = 1$  and  $B_1, B_2, B_3 = 0$ . For  $J_{12}, J_{23}, J_{31} = 0$  and  $B_1, B_2, B_3 = 1$ , the three qubits are decoupled and the degenerate ground states (in the sector with  $\sum_j \sigma_j^z = -1$ ) are

$$|\psi_1\rangle = |\uparrow\downarrow\downarrow\rangle, \quad |\psi_2\rangle = |\downarrow\uparrow\downarrow\rangle, \quad |\psi_3\rangle = |\downarrow\downarrow\uparrow\rangle. \quad (6)$$

These unentangled direct-product states are easy to prepare by single-qubit operations. We choose one of these ground states, namely  $|\psi_1\rangle$  as our initial state  $|\psi(0)\rangle$ . The target state, as a linear combination of these three degenerate ground states above, is also a ground state for  $B_1, B_2, B_3 = 1$  and  $J_{12}, J_{23}, J_{31} = 0$ . It becomes the unique ground state upon adding finite  $J_{12} = J_{23} = J_{31}$ . Nevertheless, we cannot adiabatically transform the above product states to the target state due to this exact degeneracy.

As an example, we consider a particular trajectory by setting all  $B$  parameters equal to  $1 - t/\tau$  and all the  $J$  parameters equal to  $t/\tau$ . We checked the energy gap between the ground state and first excited along this trajectory (in the 3-dimensional sector), which vanishes at  $t/\tau = 0$  due to the degeneracy mentioned above, as shown in Fig. 1(a). We quantify

the difference between the final state of the system and the target state by the cost function

$$\mathcal{E} = 1 - |\langle\psi_{\text{target}}|\psi(\tau)\rangle|^2. \quad (7)$$

The error above is nonnegative and vanishes if we reach the target state. In Fig. 1(b), we plot the error as a function of the total time  $\tau$ . The time evolution does not change the error  $\mathcal{E}$  from its initial value of  $2/3$ . The Hamiltonian with an initial  $(1, 0, 0)$  state leads to normalized final states of the form  $|\psi(\tau)\rangle = (\alpha - i\beta, 2i\beta, 2i\beta)$ , where  $\alpha$  and  $\beta$  are two real numbers, all of which have the same error  $\mathcal{E}$  with respect to the  $W$  state. It is not surprising that we cannot evolve the state adiabatically because the initial state is degenerate. Even if an adiabatic trajectory existed, adiabatic solutions only reach the target state in long timescales. Here, we wish to find a solution that reaches the target state in the minimum amount of time.

### III. PONTRYAGIN'S MINIMUM PRINCIPLE

To find the amount of time needed to reach the maximally entangled state, we calculate the smallest possible error for a fixed total time  $\tau$ . The error is a functional of the time-dependent control parameters  $B_n(t)$  and  $J_{nm}(t)$ , which can be tuned to arbitrary functions of time as long as they remain in the range specified in Eq. (3). Our goal is to minimize the error over the trajectories of all these parameters.

Pontryagin's minimum principle provides remarkable insight into the mathematical structures of the protocols that minimize the cost function. We will use it as a means of verifying and improving our numerical results. To employ Pontryagin's minimum principle, we first construct a mathematical object known as the optimal-control Hamiltonian (OCH), not to be confused with the quantum Hamiltonian that generates the physical time evolution. The OCH is defined as

$$\mathcal{H} = \mathbf{p}^T \cdot \mathbf{f}(\mathbf{x}, \{\alpha\}), \quad (8)$$

for a system with dynamical variables  $\mathbf{x}$  evolving with the equations of motion

$$\dot{\mathbf{x}} = \mathbf{f}(\mathbf{x}, \{\alpha\}), \quad (9)$$

where  $\{\alpha(t)\}$  is the set of control functions (in this case,  $B_n$  and  $J_{nm}$ ), and  $\mathbf{p}$  are conjugate momenta defined with respect to the dynamical variables  $\mathbf{x}$ . We treat  $\mathbf{x}$  and  $\mathbf{p}$  as column vector, with the superscript T indicating the matrix transpose. The conjugate momenta evolve with the Hamilton equations of motion

$$\dot{\mathbf{p}} = -\partial_{\mathbf{x}}\mathcal{H}. \quad (10)$$

The analogous  $\dot{\mathbf{x}} = \partial_{\mathbf{p}}\mathcal{H}$  is equivalent to Eq. (9). The conjugate momenta satisfy the following boundary condition:

$$\mathbf{p}(\tau) = \partial_{\mathbf{x}}\mathcal{E}(\mathbf{x}(\tau)), \quad (11)$$

where  $\mathcal{E}$  is the cost function to be minimized.

If we insert the optimal trajectories  $\mathbf{x}_{\text{opt}}$  and  $\mathbf{p}_{\text{opt}}$  corresponding to the optimal protocol into the OCH, it becomes a function of the control parameters  $\{\alpha\}$ . The optimal  $\alpha_{\text{opt}}$  then minimizes the OCH at every point in time

$$\mathcal{H}(\mathbf{x}_{\text{opt}}, \mathbf{p}_{\text{opt}}, \{\alpha_{\text{opt}}\}) = \min_{\{\alpha\}} \mathcal{H}(\mathbf{x}_{\text{opt}}, \mathbf{p}_{\text{opt}}, \{\alpha\}). \quad (12)$$

To apply this formalism to the problem at hand, we first derive the OCH for the system. The state of the system can be represented by a three-dimensional complex vector  $|\psi(t)\rangle = \mathbf{R} + i\mathbf{I}$ , where  $\mathbf{R}$  and  $\mathbf{I}$ , the real and imaginary parts of the quantum state, are three-dimensional real vectors. Since the Hamiltonian  $H$  in Eq. (5) is real, the Schrödinger equation reduces to the following equations of motion for the dynamical variables  $\mathbf{R}$  and  $\mathbf{I}$ :

$$\dot{\mathbf{R}} = H(t)\mathbf{I}, \quad \dot{\mathbf{I}} = -H(t)\mathbf{R}. \quad (13)$$

The OCH can then be written as

$$\mathcal{H} = \mathbf{P}_{\mathbf{R}}^T H(t)\mathbf{I} - \mathbf{P}_{\mathbf{I}}^T H(t)\mathbf{R}, \quad (14)$$

where  $\mathbf{P}_{\mathbf{R}}$  and  $\mathbf{P}_{\mathbf{I}}$  respectively denote the conjugate momenta to the dynamical variable vectors  $\mathbf{R}$  and  $\mathbf{I}$ . By combining the above real conjugate momenta into a complex vector

$$|\Pi\rangle = \mathbf{P}_{\mathbf{R}} + i\mathbf{P}_{\mathbf{I}}, \quad (15)$$

we can write the OCH in the compact form

$$\mathcal{H} = \text{Im}[\langle \Pi(t) | H(t) | \psi(t) \rangle] \quad (16)$$

From the equations of motion (10), we find that  $|\Pi\rangle$  also satisfies the Schrodinger equation

$$\partial_t |\Pi(t)\rangle = -iH(t)|\Pi(t)\rangle. \quad (17)$$

Unlike the quantum state  $|\psi(t)\rangle$ , for which the boundary conditions are given at the initial time  $t = 0$ , the Pontryagin's theory specifies a boundary condition for  $|\Pi(t)\rangle$  at the final time  $t = \tau$  through Eq. (11), which depends on the cost function. Using the error function (7) with  $\langle \psi_{\text{target}} |$  represented by  $(1/\sqrt{3}, 1/\sqrt{3}, 1/\sqrt{3})$ , we find

$$\mathcal{E} = 1 - \frac{1}{3} \langle \psi(\tau) | \mathcal{M} | \psi(\tau) \rangle, \quad \mathcal{M} \equiv \begin{pmatrix} 1 & 1 & 1 \\ 1 & 1 & 1 \\ 1 & 1 & 1 \end{pmatrix}. \quad (18)$$

The above expression leads to the following boundary condition:

$$|\Pi(\tau)\rangle = -\frac{2}{3} \mathcal{M} | \psi(\tau) \rangle. \quad (19)$$

Suppose we have a dynamical protocol for the Hamiltonian parameters  $B_n(t)$  and  $J_{nm}(t)$ . Since we know the initial conditions for  $|\psi\rangle$ , we can determine  $|\psi(t)\rangle$  for all times. Then the boundary condition (19) gives the final value of  $|\Pi\rangle$ , and we can solve the Schrödinger equation backward in time and find  $|\Pi(t)\rangle$ . Then, using Eq. (16), we obtain the functional dependence of the OCH on the Hamiltonian parameters.

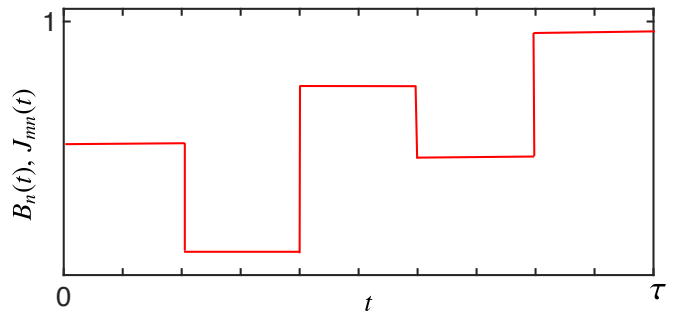


FIG. 2. An example of what a single parameter's protocol may look like for an  $N = 5$  optimization. The value of every step in the protocol for each parameter is given as an input to the error minimization algorithm and allowed to be between 0 and 1.

Importantly, since the elements of  $H(t)$  have a linear dependence on  $B_n(t)$  and  $J_{nm}(t)$ , the OCH (16) is a linear function of these parameters. Minimizing the OCH (16) over the control parameters then generically yields bang-bang protocols. As an example, if the coefficient of  $B_1$  in the OCH is positive (negative), we must set  $B_1$  to its minimum (maximum) allowed value  $B_1 = 0$  ( $B_1 = \Lambda$ ). The only exception is through the so-called singular intervals, for which the coefficients above identically vanish over a finite interval.

To determine the above coefficient, again we use  $B_1$  as an example and write

$$\partial_{B_1} \mathcal{H} = \text{Im}[\langle \Pi(t) | \mathcal{K}_{B_1} | \psi(t) \rangle] \quad (20)$$

Where  $\mathcal{K}_{B_1}$  denotes the partial derivative of the Hamiltonian (5) with respect to  $B_1$ . In this particular case, it is a diagonal matrix with elements  $+1$ ,  $-1$ , and  $-1$  on the diagonal.

These OCH coefficients can be used to check whether a given (bang-bang) protocol is optimal. As mentioned above, given a protocol, we can find the corresponding  $|\psi\rangle$  and  $|\Pi\rangle$  as a function of time. Thus, given a protocol, we can determine  $\partial_{B_n} \mathcal{H}$  and  $\partial_{J_{nm}} \mathcal{H}$  as a function of time. The jumps in the bang-bang protocol coincide with changes in the signs of these coefficients. If a protocol is optimal and minimizes the OCH, the parameters are at their maximum (minimum) value when the corresponding OCH coefficient is negative (positive).

The Pontryagin's theorem provides a powerful iterative approach to finding the numerically exact optimal protocol. The only drawback is that if the initial guess is not close to the optimal protocol, the iterations do not converge. Thus a preliminary numerical optimization is necessary to find the approximate optimal protocols. As discussed below, we use a two-stage optimization. After inferring the number of jumps from a rough brute-force optimization, to speed up the numerical optimization, we assume the appropriate bang-bang structure.

## IV. NUMERICAL OPTIMIZATION

### A. Piecewise-constant optimization

For a brute-force approach, it is necessary to turn the error functional into a multivariable function. We first divide the total time ( $\tau$ ) into  $N$  intervals of length  $\tau/N$  as shown in Fig. 2 for  $N = 5$ . In the limit of  $N \rightarrow \infty$ , we can approximate any permissible control parameter by a piecewise-constant function over these  $N$  intervals. By starting with a finite  $N$  and slowly increasing it, we can learn the general shape of the protocol and find numerically exact results by a secondary optimization based on Pontryagin's minimum principle. We then write the final state as

$$|\psi(\tau)\rangle = U_N(\tau - t_{N-1})U_{N-1}(t_{N-1} - t_{N-2})\dots U_1(t_1)|\psi(0)\rangle. \quad (21)$$

Over each of these intervals, the  $B_n(t)$  ( $n = 1, 2, 3$ ) and  $J_{nm}(t)$  ( $nm = 12, 23, 31$ ) parameters are allowed to be any constant value within the specified range (3). The value of these parameters for all intervals determines the unitary evolution matrices, which in turn determine the error of the protocol. Hence  $\mathcal{E}$  is a multivariable function of  $6N$  control variables. We then use an interior point algorithm to minimize the error for these  $6N$  numbers. These simulations did not converge to clean bang-bang protocols, likely due to coarse discretization and the presence of many local minima. However, the number of ups and downs in the protocols suggested a maximum of three discontinuous jumps for each control parameter. We then performed bang-bang optimization, by allowing a maximum of three jumps (in the spirit of quantum approximate optimization algorithm), as discussed below. Indeed we found that our optimal bang-bang protocols indeed do not have more than two jumps, and outperform the results of the initial brute-force minimization.

### B. Bang-Bang optimization

Despite convergence difficulties of the brute-force approach, we extracted a conjectured upper bound on the number of jumps. We then used an optimization method that assumes a bang-bang protocol to minimize the error for the switching times of the parameters. The variables of the program were the times at which those switches happened. The unitary evolution has a similar structure as the piecewise-constant optimization, but the parameters were only allowed to be their maximum or minimum values (one or zero) during each interval. The intervals were not necessarily of equal duration.

We used the simulated annealing algorithm (a global optimization algorithm designed to escape local minima) to minimize the error function  $\mathcal{E}$ . An example of a solution for  $\tau = 0.55$  is shown in Fig. 3. The solid blue lines indicate the Hamiltonian parameter as a function of time. In this particular case, the parameters  $B_1$ ,  $B_2$ , and  $J_{12}$  are turned off throughout

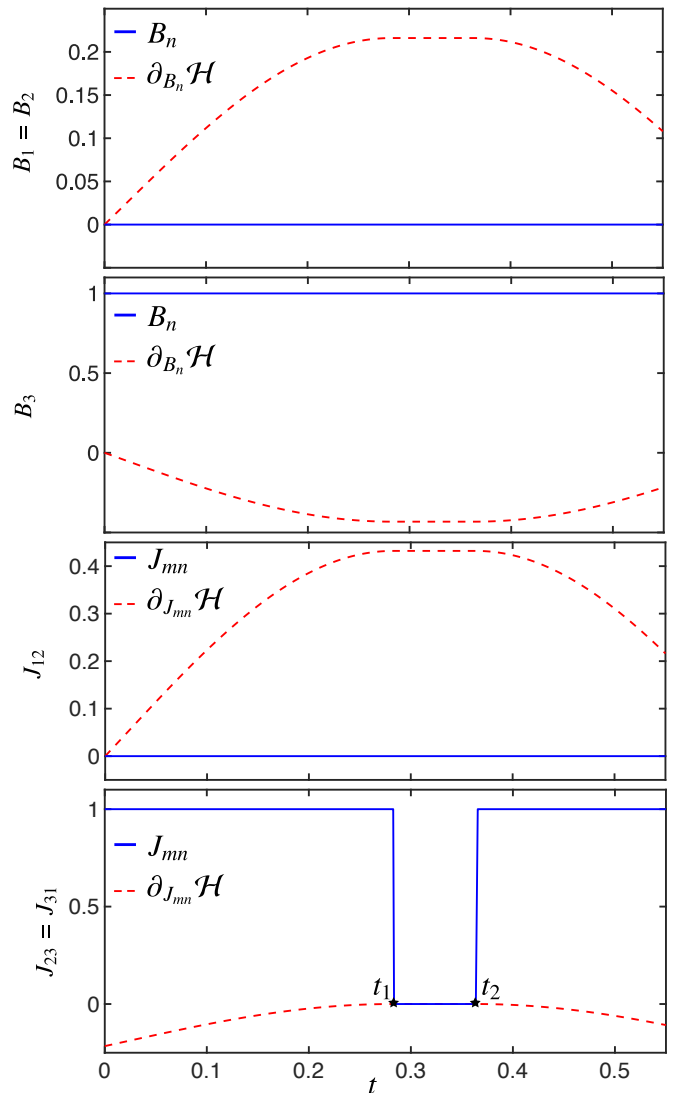


FIG. 3. Optimal protocols (from the bang-bang optimization) for all control parameters for  $\tau = 0.55$  plotted along with their OCH coefficients.

the evolution, the parameter  $B_3$  is on during the evolution, and  $J_{23} = J_{31}$  is initially on, turned off for a finite time, and turned on again. We were able to confirm and improve our solutions with Pontryagin's minimum principle, as discussed in the section below.

### C. Confirmation of optimal protocols with Pontryagin minimum principle

To confirm the protocols found using the simulated annealing algorithm, we used the Pontryagin's minimum principle. Although the protocols are already very accurate, an iteration with the Pontragin's theorem makes them even more precise. As stated before, we can check whether we have found the optimal protocol by solving for the OCH,  $\mathcal{H}$ , and the coeffi-

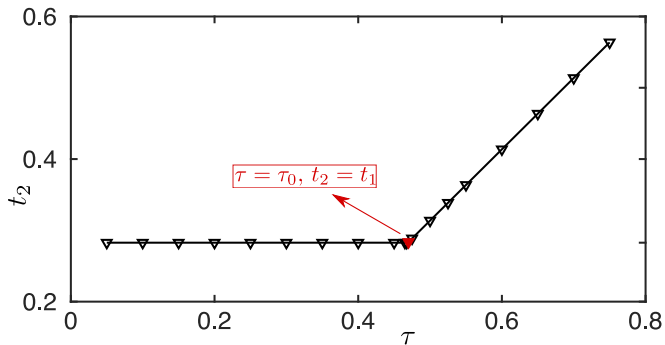


FIG. 4. The second switching time,  $t_2$  in the optimal protocols for the  $J_{23}$  and  $J_{31}$  parameters as a function of the total time  $\tau$  (the first switching time stays constant at  $t_1 = 0.282687$ ). For  $\tau > \tau_0$  the second switching time exhibits a linear dependence on  $\tau$  with a slope of 1.

coefficients such as  $\partial_{J_{23}} \mathcal{H} = \text{Im}[\langle \Pi(t) | \mathcal{K}_{J_{23}} | \psi(t) \rangle]$  [see Eq. (20)] as a function of time for a given protocol. To minimize the OCH, we must keep the parameter at its maximum (minimum) value while it's coefficient is negative (positive). Thus, the coefficients for each  $B_n$  and  $J_{nm}$  parameter in the OCH should pass through zero at the same time that the parameter switches between maximum and minimum values.

In Fig. 3, we show the corresponding coefficient (dashed red line) to each of the control parameters, calculated with the method above (see the Appendix for more details). All results are consistent with the Pontryagin's theorem. For the constant protocols  $J_{12}$  and  $B_{1,2,3}$ , the sign of the coefficient agrees with the value of the control parameter. For  $J_{23} = J_{31}$ , the coefficient is negative when the control parameter is equal to one. Interestingly, the finite interval with a vanishing control parameter has a coefficient that is identically zero. Similar behavior occurs for the optimal preparation of the maximally entangled state of two qubits; there are *singular* intervals, where the Pontryagin's theorem does not determine the protocol. A priori, optimal protocols do not need to be bang-bang if singular intervals are present. However, in this case, it seems that the optimal protocol is nevertheless bang-bang.

We found that for  $0 \leq \tau \leq \tau_0 = 0.469017$ , all the control parameters are constant through the entire evolution. For larger  $\tau$ , a single dip appears in  $J_{23}$  and  $J_{31}$  at time  $t_1 = 0.282687$ . A second jump appears at a time  $t_2$  with  $t_1 \leq t_2 < \tau$ . We can put these two patterns on the same footing by setting  $t_2 = t_1$  for  $0 \leq \tau \leq \tau_0$ . All intervals are nonsingular except for the  $t_1 < t < t_2$  singular interval.

While  $t_1$  is independent of  $\tau$ , as seen from Fig. 4,  $t_2$ , the time of the second switch in the protocol for  $J_{23}$  and  $J_{31}$  parameters, depends linearly on  $\tau$ . We quantify this relationship by investigating the evolution of the OCH coefficients of these parameters. Let us write  $t_2$  as a function of  $\tau$  as

$$t_2(\tau) = (\tau - \tau_0) + t_1 \quad (\tau \geq \tau_0), \quad (22)$$

where we found a slope of 1 by a linear fit of the numerical data in Fig. 4.

The pattern shown in Fig. 3 together with Eq. (22) and the

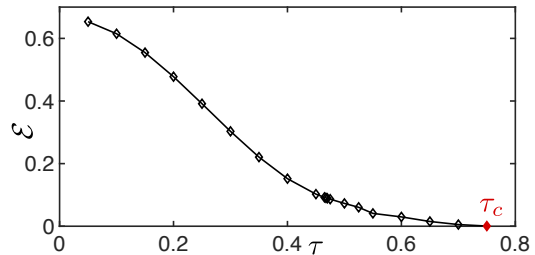


FIG. 5. The minimum error (corresponding to the optimal protocol) between the final state and maximally entangled state as a function of the total time  $\tau$ .

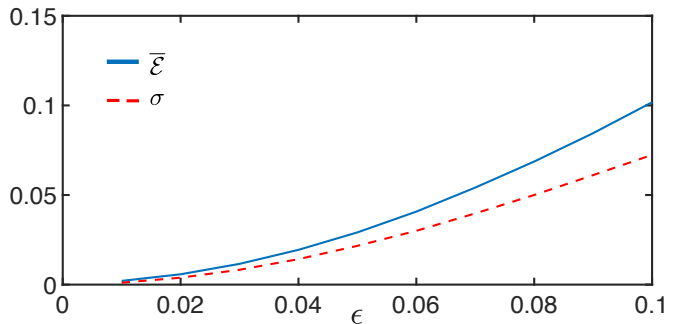


FIG. 6. The average final error and its standard deviation as a function of the timing error  $\epsilon$ .

fixed values of  $t_1$  and  $\tau_0$  uniquely determine the optimal protocol for any total time  $\tau$ . The next question is, what is the minimum  $\tau$ , for which the optimal protocol can prepare the  $W$  state exactly. By scanning over a range of final times, we have determined that the desired maximally entangled state is reached in a finite amount of time. As seen in Fig. 5, for  $\tau \geq \tau_c \approx 0.77$ , the error between the final state and the desired state becomes negligible. Since we know the bang-bang pattern of the optimal protocol, we can determine the precise value of  $\tau_c$  by writing the error  $\mathcal{E}$  analytically in terms of  $\tau$ , as shown in the Appendix, which leads to  $\tau_c = 0.7727$ . The bang-bang protocols we have found reach the maximally entangled state of three qubits in a short time of order unity (in natural units determined by the energy scale  $\Lambda$  (3)).

## V. STABILITY OF OPTIMAL SOLUTIONS

When implementing these optimal protocols in an experimental setting, there will be some unavoidable inaccuracy in switching the parameters on or off at the optimal times. It is thus essential to investigate the effect on the final error. We introduce random errors drawn from a uniform distribution  $[-\epsilon/2, \epsilon/2]$  to each of the switching times of the optimal protocols. We work with the optimal protocols found at  $\tau = 0.75$ , where the final errors for a perfect protocol are negligible (of order  $10^{-5}$ ). Upon perturbing the optimal protocol

by these shifts in the switching time, we calculate the final error,  $\mathcal{E}$  for each realization. We found that  $10^4$  realizations are enough to obtain convergence for both the average,  $\overline{\mathcal{E}}$ , and the standard deviation  $\sigma$  of the final error. Here the overline indicates averaging over the realization of timing inaccuracies, and  $\sigma = \sqrt{\overline{\mathcal{E}^2} - (\overline{\mathcal{E}})^2}$ .

The results of this calculation are shown in Fig 6. Both the average error and its standard deviation grow slowly are still negligible for timing errors of order 2%. Typical timing error realizations thus yield negligible errors in the final wavefunction.

## VI. CONCLUSION

Within the superconducting gmon qubit architecture [22] we have found optimal protocols that maximally entangle a system of three qubits in a finite amount of time. These protocols turned out to be simple bang-bang protocols where parameters were turned on and off at specific optimal times. Each bang corresponds to a specific unitary operation that can be performed by manipulating the voltage across the inductor that couples our gmon qubits in the superconducting system (to learn more about what these operations correspond to see Ref. [22]). During experiment the amount of time needed for this process can be made arbitrarily small by increasing the energy scale (3) of the system. The ability to tune the time scale for these protocols leaves room for many other processes to be completed before the system decoheres which make them very useful for information processing in a quantum computer. Comparing our results with those of Bao et al. [45] we can see that the protocols required to maximally entangle a system of three qubits contain an additional switch than the protocols that maximally entangle a system of two qubits. Our prevailing bang-bang structure during the time when the OCH coefficient becomes singular is also consistent with the results of Bao et al. [45]. These singularities may cause some difficulties in proving an optimal protocol for increasing numbers of qubits. Further work will generalize these results for the second class of maximally entangled states of a three qubit system, different initial states, and greater numbers of qubits to investigate the effect that each of these has on the optimal protocols for maximally entangling the system.

### Appendix A: Pontryagin coefficient for the singular interval

With the patterns discovered above we can write the wavefunction as

$$\begin{aligned} |\psi(t)\rangle &= U_1(t)|\psi_0\rangle, & t < t_1, \\ |\psi(t)\rangle &= U_2(t-t_1)U_1(t_1)|\psi_0\rangle, & t_1 < t < t_2, \\ |\psi(t)\rangle &= U_1(t-t_2)U_2(t_2-t_1)U_1(t_1)|\psi_0\rangle, & t_2 < t < \tau, \end{aligned} \quad (\text{A1})$$

where  $U_j(t) = e^{-iH_j}$  for  $j = 1, 2$  and

$$H_1 \equiv H(B_1 = B_2 = J_{12} = 0, B_3 = 1, J_{23} = J_{31} = 1), \quad (\text{A2})$$

$$H_2 \equiv H(B_1 = B_2 = J_{12} = 0, B_3 = 1, J_{23} = J_{31} = 0). \quad (\text{A3})$$

We then find that  $U_2$  is a diagonal matrix  $U_2(t) = \text{diag}(e^{-it}, e^{it}, e^{it})$  and  $U_1(t)$  is given by the matrix

$$\begin{pmatrix} c_3 + \frac{1}{3}is_3 & \frac{2}{3}is_3 & \frac{2}{3}is_3 \\ \frac{2}{3}is_3 & \frac{1}{2}c_1 + \frac{1}{2}c_3 - \frac{1}{2}is_1 - \frac{1}{6}is_3 & -2c_1c_1^2 + \frac{2}{3}ic_1^3 \\ \frac{2}{3}ic_3 & -2c_1s_1^2 + \frac{2}{3}is_1^3 & \frac{1}{2}c_1 + \frac{1}{2}c_3 - \frac{1}{2}is_1 - \frac{1}{6}is_3 \end{pmatrix},$$

where we have introduced the shorthand notation  $c_n \equiv \cos(nt)$  and  $s_n \equiv \sin(nt)$ . Using the boundary condition (19), we can similarly write expressions for the conjugate momenta:

$$|\Pi(t)\rangle = -\frac{2}{3}U_1^\dagger(\tau-t)\mathcal{M}|\psi(\tau)\rangle, \quad t_2 < t < \tau, \quad (\text{A4})$$

$$|\Pi(t)\rangle = -\frac{2}{3}U_2^\dagger(t_2-t)U_1^\dagger(\tau-t_2)\mathcal{M}|\psi(\tau)\rangle, \quad t_1 < t < t_2,$$

$$|\Pi(t)\rangle = -\frac{2}{3}U_1^\dagger(t_1-t)U_2^\dagger(t_2-t_1)U_1^\dagger(\tau-t_2)\mathcal{M}|\psi(\tau)\rangle, \quad t < t_1,$$

The above expressions for the quantum state and the conjugate momenta allow us to calculate  $\partial_J \mathcal{H}$  and  $\partial_B \mathcal{H}$  as a function of time, using Eq. (20) and its analogs for other control parameters.

Focusing on the singular interval  $t_1 < t < t_2$ , let us, as an example, determine  $\partial_{J_{23}} \mathcal{H} = \text{Im}\langle \Pi(t) | \mathcal{K}_{J_{23}} | \psi(t) \rangle$ , where

$$\begin{aligned} \langle \Pi(t) | \mathcal{K}_{J_{23}} | \psi(t) \rangle &= -\frac{2}{3} \langle \psi(0) | U_1^\dagger(t_1) U_2^\dagger(t_2-t_1) U_1^\dagger(\tau-t_2) \\ &\quad \mathcal{M} U_1(\tau-t_2) U_2(t_2-t) \mathcal{K}_{J_{23}} U_2(t-t_1) U_1(t_1) | \psi(0) \rangle \end{aligned}$$

We can explicitly write the above expression by using

$$\mathcal{K}_{J_{23}} = \begin{pmatrix} 0 & -2 & 0 \\ -2 & 0 & 0 \\ 0 & 0 & 0 \end{pmatrix}, \quad |\psi(0)\rangle = \begin{pmatrix} 1 \\ 0 \\ 0 \end{pmatrix}. \quad (\text{A5})$$

The imaginary part of  $\langle \Pi(t) | \mathcal{K}_{J_{23}} | \psi(t) \rangle$  above is a length trigonometric expression, which can be calculated explicitly. It turns out that for the values of  $t_1$  and  $\tau_0$ , this function vanishes for all  $t$  and  $\tau$ , indicating the singularity of the interval. It is important to emphasize that the above analytical expressions depend on the particular bang-bang form of the optimal protocol, which we obtained through numerical optimization. However, now that the pattern is known, we can use these analytical expressions to fine the values of  $t_1$  and  $\tau_0$  with extreme precision. To determine  $\tau_c$ , we can then directly write the error  $\mathcal{E}$  in terms of  $\tau$  (again for our particular pattern with fixed  $\tau_0$  and  $t_1$ ) and see when it first vanishes by writing the overlap as

$$\langle \psi_{\text{target}} | \psi(\tau) \rangle = \langle \psi_{\text{target}} | U_1(\tau_0-t_1) U_2(\tau-\tau_0) U_1(t_1) | \psi_0 \rangle, \quad (\text{A6})$$

which yields explicit trigonometric expressions.

## ACKNOWLEDGMENTS

This work was supported by the National Science Foundation Award No. DMR-1945395. AR is grateful to the Kavli Institute for Theoretical Physics for hospitality during the completion of this work, supported in part by the National Science Foundation under Grant No. PHY-1748958.

- 
- [1] D. D. Awschalom, L. C. Bassett, A. S. Dzurak, E. L. Hu, and J. R. Petta, *Science* **339**, 1174 (2013).
- [2] C. Monroe and J. Kim, *Science* **339**, 1164 (2013).
- [3] M. H. Devoret and R. J. Schoelkopf, *Science* **339**, 1169 (2013).
- [4] M. A. Nielsen and I. L. Chuang, *Quantum Computation and Quantum Information* (Cambridge Univ. Press, 2000).
- [5] T. D. L. et al, *Nature* **464**, 45 (2010).
- [6] S. Tamaryan, T.-C. Wei, and D. Park, *Phys. Rev. A* **80**, 052315 (2009).
- [7] W. Dür, G. Vidal, and J. I. Cirac, *Phys. Rev. A* **62**, 062314 (2000).
- [8] Y.-H. Chen, B.-H. Huang, J. Song, and Y. Xia, *Opt. Comm.* **380**, 140 (2016).
- [9] N. B. An, *Phys. Lett. A* **344**, 77 (2005).
- [10] S.-B. Zheng, *Journal of Optics B: Quantum and Semiclassical Optics* **7**, 10 (2004).
- [11] Y.-H. Kang, Y. Xia, and P.-M. Lu, *J. Opt. Soc. Am. B* **32**, 1323 (2015).
- [12] M. Eibl, N. Kiesel, M. Bourennane, C. Kurtsiefer, and H. Weinfurter, *Phys. Rev. Lett.* **92**, 077901 (2004).
- [13] X. Zou, K. Pahlke, and W. Mathis, *Phys. Rev. A* **66**, 044302 (2002).
- [14] P. Watts, J. Vala, M. M. Müller, T. Calarco, K. B. Whaley, D. M. Reich, M. H. Goerz, and C. P. Koch, *Phys. Rev. A* **91**, 062306 (2015).
- [15] M. H. Goerz, G. Gualdi, D. M. Reich, C. P. Koch, F. Motzoi, K. B. Whaley, J. c. v. Vala, M. M. Müller, S. Montangero, and T. Calarco, *Phys. Rev. A* **91**, 062307 (2015).
- [16] X. Wei and M. F. Chen, *Int. J. Theor. Phys.* **54**, 812 (2015).
- [17] F. Helmer and F. Marquardt, *Phys. Rev. A* **79**, 052328 (2009).
- [18] K.-H. Song, Z.-W. Zhou, and G.-C. Guo, *Phys. Rev. A* **71**, 052310 (2005).
- [19] Z. J. Deng, K. L. Gao, and M. Feng, *Phys. Rev. A* **74**, 064303 (2006).
- [20] Y.-H. Kang, Y.-H. Chen, Q.-C. Wu, B.-H. Huang, J. Song, and Y. Xia, *Sci. Rep.* **6**, 36737 (2016).
- [21] M. Neeley, R. C. Bialczak, M. Lenander, E. Lucero, M. Mariantoni, A. D. O'Connell, D. Sank, H. Wang, M. Weides, J. Wenner, Y. Yin, T. Yamamoto, A. N. Cleland, and J. M. Martinis, *Nature* **467**, 570 EP (2010).
- [22] Y. Chen, C. Neill, P. Roushan, N. Leung, M. Fang, R. Barends, J. Kelly, B. Campbell, Z. Chen, B. Chiaro, A. Dunsworth, E. Jeffrey, A. Megrant, J. Y. Mutus, P. J. J. O'Malley, C. M. Quintana, D. Sank, A. Vainsencher, J. Wenner, T. C. White, M. R. Geller, A. N. Cleland, and J. M. Martinis, *Phys. Rev. Lett.* **113**, 220502 (2014).
- [23] C. Brif, R. Chakrabarti, and H. Rabitz, *New Journal of Physics* **12**, 075008 (2010).
- [24] J. Werschnik and E. K. U. Gross, *Journal of Physics B: Atomic, Molecular and Optical Physics* **40**, R175 (2007).
- [25] E. Torrontegui, S. Ibáñez, S. Martínez-Garaot, M. Modugno, A. del Campo, D. Guéry-Odelin, A. Ruschhaupt, X. Chen, and J. G. Muga, in *Advances in Atomic, Molecular, and Optical Physics*, Advances In Atomic, Molecular, and Optical Physics, Vol. 62, edited by E. Arimondo, P. R. Berman, and C. C. Lin (Academic Press, 2013) pp. 117 – 169.
- [26] A. del Campo, *EPL (Europhysics Letters)* **96**, 60005 (2011).
- [27] X. Chen, A. Ruschhaupt, S. Schmidt, A. del Campo, D. Guéry-Odelin, and J. G. Muga, *Phys. Rev. Lett.* **104**, 063002 (2010).
- [28] C. Jarzynski, *Phys. Rev. A* **88**, 040101 (2013).
- [29] P. Salamon, K. H. Hoffmann, Y. Rezek, and R. Kosloff, *Phys. Chem. Chem. Phys.* **11**, 1027 (2009).
- [30] G.-Q. Li, G.-D. Chen, P. Peng, and W. Qi, *The European Physical Journal D* **71**, 14 (2017).
- [31] S. Choi, R. Onofrio, and B. Sundaram, *Phys. Rev. A* **84**, 051601 (2011).
- [32] J. P. Palao and R. Kosloff, *Phys. Rev. Lett.* **89**, 188301 (2002).
- [33] K. H. Hoffmann, P. Salamon, Y. Rezek, and R. Kosloff, *EPL (Europhysics Letters)* **96**, 60015 (2011).
- [34] A. Rahmani and C. Chamon, *Phys. Rev. Lett.* **107**, 016402 (2011).
- [35] P. Doria, T. Calarco, and S. Montangero, *Phys. Rev. Lett.* **106**, 190501 (2011).
- [36] T. Caneva, T. Calarco, R. Fazio, G. E. Santoro, and S. Montangero, *Phys. Rev. A* **84**, 012312 (2011).
- [37] A. P. Peirce, M. A. Dahleh, and H. Rabitz, *Phys. Rev. A* **37**, 4950 (1988).
- [38] R. Kosloff, S. Rice, P. Gaspard, S. Tersigni, and D. Tannor, *Chemical Physics* **139**, 201 (1989).
- [39] A. Rahmani, B. Seradjeh, and M. Franz, *Phys. Rev. B* **96**, 075158 (2017).
- [40] K. Ritland and A. Rahmani, *New J. Phys.* **20**, 065005 (2018).
- [41] U. Hohenester, P. K. Rekdal, A. Borzi, and J. Schmiedmayer, *Phys. Rev. A* **75**, 023602 (2007).
- [42] W. Rohringer, R. Bücker, S. Manz, T. Betz, C. Koller, M. Göbel, A. Perrin, J. Schmiedmayer, and T. Schumm, *Applied Physics Letters* **93**, 264101 (2008).
- [43] S. E. Sklarz, D. J. Tannor, and N. Khaneja, *Phys. Rev. A* **69**, 053408 (2004).
- [44] A. Rahmani, *Modern Physics Letters B* **27**, 1330019 (2013).
- [45] S. Bao, S. Kleer, R. Wang, and A. Rahmani, *Phys. Rev. A* **97**, 062343 (2018).